








BRIEF REPORT | FEBRUARY 23 2022

Simulated effect of edge plasma density parameters on lower hybrid wave scattering in EAST **FREE**

C. B. Wu ; B. J. Ding  ; S. G. Baek ; M. H. Li ; G. M. Wallace ; Y. C. Li; G. H. Yan 



Physics of Plasmas 29, 024503 (2022)

<https://doi.org/10.1063/5.0077657>

 CHORUS



View
Online



Export
Citation

CrossMark

Articles You May Be Interested In

Modeling the spectral modification of lower hybrid wave in the presence of drift-wave type density fluctuation in the scrape-off-layer of the EAST tokamak

Physics of Plasmas (August 2021)

Characterization of onset of parametric decay instability of lower hybrid waves

AIP Conference Proceedings (February 2014)

Characterization of the onset of ion cyclotron parametric decay instability of lower hybrid waves in a diverted tokamak

Physics of Plasmas (June 2014)

Simulated effect of edge plasma density parameters on lower hybrid wave scattering in EAST

Cite as: Phys. Plasmas **29**, 024503 (2022); doi: [10.1063/5.0077657](https://doi.org/10.1063/5.0077657)

Submitted: 4 November 2021 · Accepted: 11 January 2022 ·

Published Online: 23 February 2022









View Online



Export Citation



CrossMark

C. B. Wu,^{1,2}  B. J. Ding,^{1,a)}  S. C. Baek,³  M. H. Li,¹  G. M. Wallace,³  Y. C. Li,⁴ and G. H. Yan^{1,2} 

AFFILIATIONS

¹Institute of Plasma Physics, Hefei Institutes of Physical Science, Chinese Academy of Sciences, Hefei 230031, People's Republic of China

²University of Science and Technology of China, Hefei 230026, People's Republic of China

³MIT Plasma Science and Fusion Center, Cambridge, Massachusetts 02139, USA

⁴College of Optoelectronic Engineering, Shenzhen University, Shenzhen 518060, China

^{a)} Author to whom correspondence should be addressed: bjding@ipp.ac.cn

ABSTRACT

The incorporation of lower hybrid (LH) wave spectrum broadening in the poloidal wavenumber (k_θ) space at the last close field surface (LCFS) is reported to lead to better agreement of the modeled LH wave current profile with the experimental results [Baek *et al.*, Nucl. Fusion **61**, 106034 (2021)]. To further understand its underlying mechanism and find the possible influence factors, effects of wave scattering caused by drift-wave type density fluctuation on the probability distribution of the LH wave polar refractive index (N_θ) at the LCFS are studied under density parameters in the scrape-off-layer. According to a scattering model [P. T. Bonoli and E. Ott, Phys Fluids **25**(2), 359–375 (1982)], scattering probability and scattering angle distribution are two main factors that determine the degree of spectral broadening. Studies presented here show that the total scattering probability increases first and then decreases as the wave propagates toward a smaller normalized radius of poloidal magnetic flux (ρ). The degree of spectral broadening is found to depend on the density and density fluctuation together by changing the intensity and a proportion of the geometrical optics approximation term and the $E \times B$ drift term in the scattering model. Furthermore, the fluctuation correlation length can significantly modify the probability distribution of N_θ at the LCFS, which is found to significantly change the LH wave current profile.

Published under an exclusive license by AIP Publishing. <https://doi.org/10.1063/5.0077657>

In the present steady-state tokamak, the lower hybrid current drive (LHCD) has a number of advantages, such as the control of the current density profiles,¹ safety factor profile,^{2,3} neoclassical tearing modes (NTMs),⁴ and so on. At the same time, LHCD efficiency decreases sharply at high density,⁵ possibly due to strong interactions between the LH wave and the scrape-off layer (SOL).^{5–10} One possible cause is wave scattering induced by density fluctuation, which has been studied in both simulation^{11–17} and experiment. The study on Alcator C-Mod suggested that drift-wave type density fluctuation can either enhance or inhibit the penetration of the LH wave.¹⁸ The study on Tore Supra showed that the time-averaged LH current density profile is only slightly broader and shifted inward by the effect of fluctuation.¹⁹ Studies on FTU indicated that the SOL conditions could affect LHCD efficiency,²⁰ but it is difficult to distinguish between wave scattering and parametric decay instability (PDI).^{6,10} According to recent

results,^{21–24} the effects of wave scattering on LH spectrum broadening at the last close field surface (LCFS) can lead to better agreement between the experimental and simulated current profiles. The LH spectrum broadening caused by wave scattering is related to the LH wave and plasma parameters in the edge region. However, possible influence factors and the trends of wave spectrum broadening under different LH wave parameters and plasma parameters need to be studied. In our previous work, the probability distributions of $N_{||}$ and N_θ at the LCFS using different LH wave conditions have been studied with the LH_scatter module,²⁵ which is based on the LH propagation model^{26,27} and Bonoli and Ott's model.^{13,14} The LH_scatter module was used to analyze the broadening of the LH wave spectrum caused by the interaction between the LH wave and density fluctuations in the SOL.²⁵ The previous results have shown that frequency and initial $N_{||}$ can greatly broaden the probability distribution of N_θ , while there

is a little broadening in the N_{\parallel} spectrum. It was further found that the N_{θ} spectrum broadening evaluated at the LCFS broadened the LH wave driven current density profile, and the model hard x-ray (HXR) count rate profile is more consistent with the experimental result than in the case of no scattering event ($N_{\theta} = 0$).²⁵

In this paper, the LH_scatter module is used to study the effects of plasma density parameters, namely, plasma density and density fluctuation scattering length, on scattering. The total probability of scattering [$p = \sum_{\sigma} \int_{-\pi}^{\pi} d\beta(\Delta t P^{\sigma}(\beta))$] is determined by time interval Δt (analyzed in the previous work²⁵) and the scattering of probability $P^{\sigma}(\beta)$ by an angle between β and $\beta + d\beta$ in which

$$P^{\sigma}(\beta) = \sum_{\sigma} \frac{2k_{\perp}^{\sigma} \langle (\delta n/n)^2 \rangle}{V_{g\perp}^{\sigma} (\partial \epsilon / \partial \omega)^2 \xi_0^2} \times \exp\left(-\frac{\xi^2}{\xi_0^2}\right) \left\{ \left[1 + 2 \frac{k_{\perp}^{\sigma 2}}{k_{tot}^2} \epsilon_{\perp} \sin^2 \frac{\beta}{2} \right]^2 + \frac{k_{\perp}^{\sigma 4}}{k_{tot}^4} \sin^2 \beta \epsilon_{xy}^2 \right\}, \quad (1)$$

where σ refers to slow wave or fast wave, k is the LH wave number, $\xi_0 = 2\pi/\lambda_c$ depends on the fluctuation correlation length (λ_c) of density fluctuation, $\epsilon_{\parallel} = 1 - \omega_{pe}^2/\omega^2 - \omega_{pi}^2/\omega^2$, $\epsilon_{\perp} = 1 + \omega_{pe}^2/\omega_{ce}^2 - \omega_{pi}^2/\omega^2$, and $\epsilon_{xy} = \omega_{pe}^2/(\omega\omega_{ce})$ are dielectric tensor elements, ω_{pe} , ω_{pi} , and ω_{ce} refer to electron plasma frequency, ion plasma frequency, and electron cyclotron frequency, respectively. In Eq. (1), the first term in the curly bracket represents the contribution of geometrical optics approximation, which ignored the effect of off diagonal components of the lower hybrid wave dielectric tensor. The second term is formed by the coupling of the $E \times B$ drift produced by the lower hybrid wave with the low-frequency density perturbation.²⁵

An example of a density profile and a density fluctuation profile is shown in Fig. 1(a), which have different trends with the increase in ρ . Therefore, ρ is scanned to study the effect of density and density fluctuation on scattering. Moreover, the LH perpendicular wave number ($k_{\perp} = \omega N_{\perp}/c$) mainly depends on the density, and there are two different types of scattering related to k_{\perp} , which are large-angle scattering ($k_{\perp} \ll \xi_0$) near the antenna and small-angle scattering ($k_{\perp} \gg \xi_0$) near the LCFS.¹² In addition, the fluctuation correlation length (λ_c) is varied in the model to study the effect of density fluctuation on N_{θ} spectrum broadening, and how N_{θ} spectrum broadening

further affects LHCD will also be studied. The WKB approximation^{22,28,29} is strict in the SOL, meaning it needs to be verified. The specific expression can be written as follows:

$$\left| \frac{N_{\perp}^2}{N^2 - \epsilon_{\perp}} \epsilon_{xy} + i \frac{N_{\parallel}^2 N_{\perp}^2}{(N_{\perp}^2 - \epsilon_{\parallel})^2} (\epsilon_{\parallel} - 1) \right| \frac{1}{k_{\perp} L} \ll 1, \quad (2)$$

where L is the scale length of equilibrium variations [$L = (|\nabla n_e/n_e|)^{-1} = \lambda_{ne}$, where λ_{ne} is the density decay length]. The detailed derivation process is given in Biswas's paper.²² The region satisfying the WKB approximation can be shown in Fig. 1(b). The position of the antenna in EAST is about $\rho \approx 1.15$. It is assumed that the slow wave is launched from the position of $\rho = 1.12$ to satisfy the WKB approximation, and the antenna-plasma coupling problem is ignored because it is difficult to distinguish from wave propagation.³⁰ In this condition, the dispersion tensor $|\mathbb{D}| < 10^{-10}$, meaning that the dispersion relation is satisfied.³¹

Based on the density and density fluctuation profiles in Fig. 1(a), the comparison of total scattering probability distribution, the contributions of both the geometrical optics approximation term and the $E \times B$ drift term to the distributions of scattering probability, and the scattering angle under different ρ are calculated as shown in Fig. 2. It is clear that the total scattering probability increases first and then decreases as the wave propagates to smaller ρ , which means that the total scattering probability has a maximum at a certain radial position (ρ_{opt}). Therefore, the total scattering probability is formed by density and density fluctuation together. As shown in Eq. (1), when $\lambda_c = 1$ cm is fixed, density fluctuation affects the magnitude of total scattering probability only, but density affects both the magnitude and shape of total scattering probability by two aspects: one is the geometrical optics approximation term, which is higher and has a smaller half-width in the case of small ρ and the other is the $E \times B$ drift term with two peaks, which is proportional to n_e^2 ($\epsilon_{xy}^2 \propto n_e^2$). According to the scattering module, the scope of scattering angle can be calculated by $\cos \beta = 1 - \xi_0^2/k_{\perp}^2$, meaning that a high density makes a narrow scope of the scattering angle. In general, the effect of density on total scattering probability is mainly reflected in the intensity and proportion of the geometrical optics approximation term and $E \times B$ drift term. With the decrease in ρ , the proportion of $E \times B$ drift term is larger and larger, while the proportion of geometrical optics approximation term is smaller and smaller.

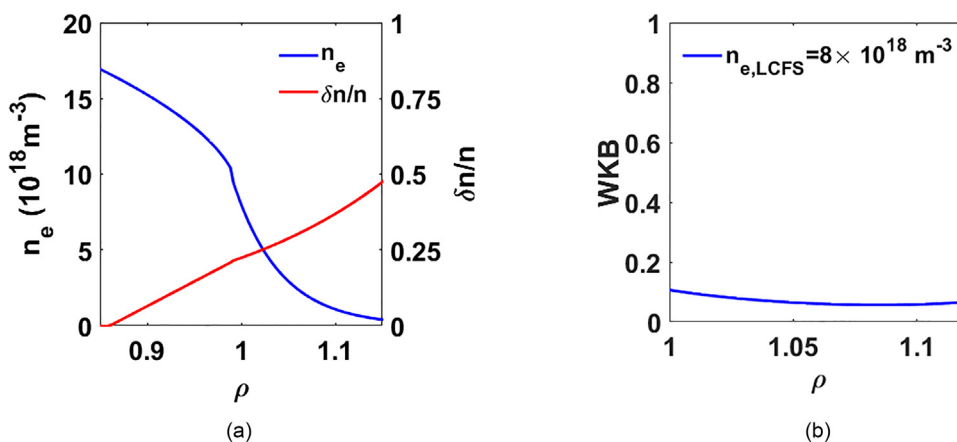


FIG. 1. (a) Density and density fluctuation profile; (b) the WKB approach validation in SOL with $\lambda_{ne} = 0.05$, $N_{\parallel} = -2.23$, and $f_{LH} = 2.45$ GHz.

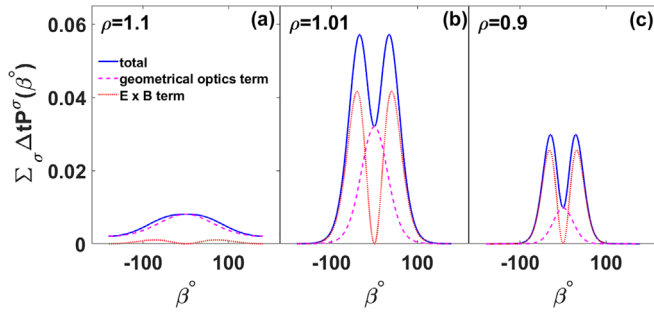


FIG. 2. Comparison of scattering probability at different ρ , where the y-axis is the total probability of scattering by an angle between β and $\beta + d\beta$. The solid blue line refers to total scattering probability, the pink dashed line refers to the contribution of geometrical optics approximation term, and the red dotted line refers to the contribution of $E \times B$ drift term. (a) $\rho = 1.1$; (b) $\rho = 1.01$; (c) $\rho = 0.9$.

In addition to density, density fluctuation parameters are also an important factor in affecting wave scattering. According to Eq. (1), the density fluctuation level only affects total scattering probability but does not affect the scattering angle. As shown in Figs. 1(a) and 2, the normalized density fluctuation level decreases at smaller ρ , but the total scattering probability increases first and then decreases, indicating that the density fluctuation level and density jointly determine the scattering probability. Regardless of the density fluctuation level, the impact of the fluctuation correlation length on the scattering probability distribution and the N_θ spectrum broadening is studied. Further, the N_θ spectrum broadening under different λ_c is used in GENRAY/CQL3D^{52,33} ray-tracing/Fokker-Planck code package to study the effect of scattering on LHCD. In order to facilitate the combination with GENRAY/CQL3D, the impact of density fluctuation within the LCFS is ignored. Based on the density and density profiles shown in Fig. 1(a), the comparison of scattering probability distribution and spectrum distribution under different λ_c is shown in Fig. 3. It indicates that the scattering angle distribution is clearly modified by λ_c . A smaller λ_c leads to a larger scattering angle, and the contribution of the $E \times B$ drift term is more important than that of the geometrical optics approximation term. It means that λ_c does not affect total scattering probability significantly but affects scattering angle distribution greatly,

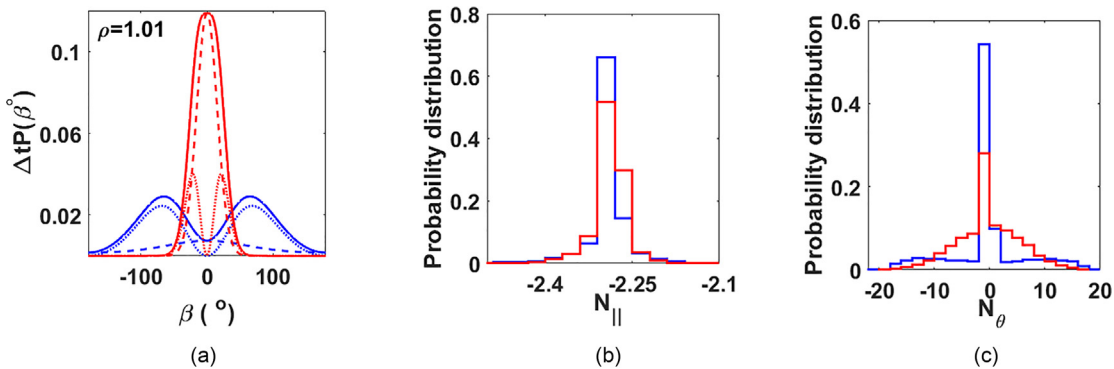


FIG. 3. (a) Scattering probability distribution over β under different λ_c ; the blue line refers to $\lambda_c = 0.5$ cm and the red line refers to $\lambda_c = 2$ cm; the type of lines is the same as Fig. 2; (b) N_{\parallel} probability distribution at the LCFS under different λ_c ; (c) N_θ probability distribution at the LCFS under different λ_c .

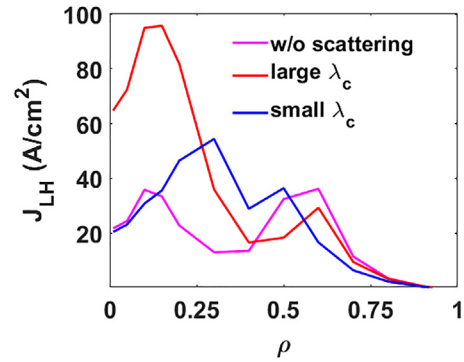


FIG. 4. Simulated LH-driven current density profile; the pink line refers to no scattering case ($N_\theta = 0$) with $I_{LH} = 150.3$ kA, the red lines refer to scattering case under $\lambda_c = 2$ cm with $I_{LH} = 176.5$ kA, and the blue lines refer to scattering case under $\lambda_c = 0.5$ cm with $I_{LH} = 164.7$ kA.

as shown in Fig. 3(a). As seen from Fig. 3(b), the N_{\parallel} probability distribution at the LCFS, which is formed by the accumulation of all scattering events on the ray trajectory from the antenna to the LCFS, is slightly broadened in both λ_c cases. The N_θ probability distribution at the LCFS is much flatter at smaller λ_c than that at larger λ_c due to the larger scattering angle probability in the case of small λ_c , as shown in Fig. 3(c).

As the N_{\parallel} spectrum broadening caused by scattering is too small to modify the ray trajectory and LHCD,²³ only the influence of different N_θ spectrum distributions at the LCFS on LHCD is considered. Two different N_θ spectrum distributions shown in Fig. 3(c) are used as initial input to the GENRAY/CQL3D in which all conditions are the same ($B_t = 2.5$ T, $I_p = 500$ kA, $\bar{n}_e = 3.5 \times 10^{19} \text{ m}^{-3}$, $n_{e,LCFS} = 8 \times 10^{18} \text{ m}^{-3}$, $T_{e0} = 1.3$ keV, $T_{e,LCFS} = 12$ eV, $V_{loop} \neq 0$, and $P_{LH} = 1$ MW) except the N_θ spectrum input to GENRAY.

Moreover, proper evolution of the electron distribution requires taking small time steps in CQL3D,^{19,22,23} which is taken between turbulence turnover time ($\tau_f = 10^{-5}$ s) and fast electron slowing-down time ($\tau_{fsd} \sim 10^{-3}$ s). Simulated LH driven current density profiles are shown in Fig. 4, which indicates that the change in the initial N_θ spectrum distribution at the LCFS has a significant effect on LHCD, and

scattering may make the LH drive current density profile larger and more inward in this case.

In summary, plasma density parameters can greatly influence scattering, which is mainly reflected in the following aspects. First, the total scattering probability increases first and then decreases with the decrease in ρ because the total scattering probability mainly depends on the density and density fluctuation together by changing the intensity and a proportion of the geometrical optics approximation term and the $\mathbf{E} \times \mathbf{B}$ drift term. Second, density plays an important role in determining the magnitude and shape of the total scattering probability distribution. The higher density leads to higher scattering probability and the narrower scattering angle, as the $\mathbf{E} \times \mathbf{B}$ drift term is proportional to n_e^2 . Third, the effect of density fluctuation on the spectral distribution shape mainly comes from the fluctuation correlation length rather than the density fluctuation level in the SOL. The fluctuation correlation length can flatten the scattering angle distribution to a great extent since the $\mathbf{E} \times \mathbf{B}$ drift term is dominant in a small fluctuation correlation length. Finally, the N_θ spectrum broadening induced by scattering may help the LH wave propagate and damp closer to the core, which is consistent with the result on Alcator C-Mod¹⁸ and Tore Supra.¹⁹ In addition, some questions need to be studied in the future, such as the density fluctuation affected by the LH wave,^{34–36} multi-pass absorption with edge reflections,³⁷ which may enhance wave scattering and make the N_θ spectrum wider,²⁵ and the power absorption and transmission coefficients of LH waves in SOL are also important,^{20,38} but it is difficult to deal with the effects of diffraction or interference in the ray trajectory. It could be clarified by full wave^{15–17,39} or particle-in-cell (PIC) methods.^{40–44}

This work was supported by the National Key Research and Development Program of China (Grant Nos. 2016YFA0400603 and 2016YFA0400602) and the National Natural Science Foundation of China (Grant Nos. 11975266, 11775259, 11675214, 11805233, and U19A20113). This work was also supported by the United States Department of Energy under Grant No. DE-SC0010492. We would like to thank Dr. P. T. Bonoli for several useful discussions concerning the scattering model formulated in Ref. 14.

AUTHOR DECLARATIONS

Conflict of Interest

The authors have no conflicts to disclose.

DATA AVAILABILITY

The data that support the findings of this study are available from the corresponding author upon reasonable request.

REFERENCES

- N. J. Fisch, *Phys. Rev. Lett.* **41**(13), 873–876 (1978).
- W. A. Houlberg, C. Gormezano, J. F. Artaud, E. Barbato, V. Basiuk, A. Becoulet, P. Bonoli, R. V. Budny, L. G. Eriksson, D. Farina, Y. Gribov, R. W. Harvey, J. Hobirk, F. Imbeaux, C. E. Kessel, V. Leonov, M. Murakami, A. Polevoi, E. Poli, R. Prater, H. S. John, F. Volpe, E. Westerhof, A. Zvonkov, ITPA Steady State Operation Topical Group, and ITPA Confinement Database and Modelling Topical Group, *Nucl. Fusion* **45**(11), 1309–1320 (2005).
- J. Garcia, G. Giruzzi, J. F. Artaud, V. Basiuk, J. Decker, F. Imbeaux, Y. Peysson, and M. Schneider, *Phys. Rev. Lett.* **100**(25), 255004 (2008).
- R. J. La Haye, *Phys. Plasmas* **13**(5), 055501 (2006).
- G. M. Wallace, R. R. Parker, P. T. Bonoli, A. E. Hubbard, J. W. Hughes, B. L. LaBombard, O. Meneghini, A. E. Schmidt, S. Shiraiwa, D. G. Whyte, J. C. Wright, S. J. Wukitch, R. W. Harvey, A. P. Smirnov, and J. R. Wilson, *Phys. Plasmas* **17**(8), 082508 (2010).
- R. Cesario, L. Amicucci, A. Cardinali, C. Castaldo, M. Marinucci, L. Panaccione, F. Santini, O. Tudisco, M. L. Apicella, G. Calabro, C. Cianfarani, D. Frigione, A. Galli, G. Mazzitelli, C. Mazzotta, V. Pericoli, G. Schettini, A. A. Tuccillo, B. Angelini, G. Apruzzese, E. Barbato, G. Belli, W. Bin, L. Boncagni, A. Botrugno, S. Briguglio, A. Bruschi, S. Ceccuzzi, C. Centioli, S. Cirant, F. Crisanti, O. D'Arcangelo, R. De Angelis, L. D. Matteo, C. D. Troia, B. Esposito, G. Fogaccia, V. Fusco, L. Gabellieri, A. Garavaglia, E. Giovannozzi, G. Granucci, G. Grossetti, G. Grosso, F. Iannone, G. Maddaluno, D. Marocco, P. Micozzi, A. Milovanov, F. Mirizzi, G. Monari, A. Moro, S. Novak, F. P. Orsitto, M. Panella, G. Pucella, G. Ravera, E. Sternini, E. Vitale, G. Vlad, V. Zanza, M. Zerbini, F. Zonca, and the FTU Team, *Nat. Commun.* **1**, 55 (2010).
- J. P. Bizarro, J. S. Ferreira, P. Rodrigues, R. Arslanbekov, and Y. Peysson, *Phys. Rev. Lett.* **75**(20), 3780–3780 (1995).
- Y. Peysson, R. Arslanbekov, V. Basiuk, J. Carrasco, X. Litaudon, D. Moreau, and J. P. Bizarro, *Phys. Plasmas* **3**(10), 3668–3688 (1996).
- H. Takahashi, *Phys. Plasmas* **1**(7), 2254–2276 (1994).
- B. J. Ding, M. H. Li, Y. C. Li, R. Cesario, A. A. Tuccillo, R. Parker, S. G. Baek, Y. F. Wang, H. Q. Liu, J. C. Xu, M. Wang, H. C. Hu, C. B. Wu, L. Wang, H. Lian, S. Y. Lin, Y. Liu, H. L. Zhao, J. F. Shan, F. K. Liu, J. P. Qian, X. Z. Gong, J. G. Li, and B. N. Wan, *Nucl. Fusion* **58**(12), 126015 (2018).
- P. M. Bellan and K. L. Wong, *Phys. Fluids* **21**(4), 592–599 (1978).
- P. L. Andrews and F. W. Perkins, *Phys. Fluids* **26**(9), 2537–2545 (1983).
- E. Ott, *Phys. Fluids* **22**(9), 1732–1736 (1979).
- P. T. Bonoli, *Phys. Fluids* **25**(2), 359–375 (1982).
- M. Madi, Y. Peysson, J. Decker, and K. Y. Kabalan, *Plasma Phys. Controlled Fusion* **57**(12), 125001 (2015).
- C. Lau, E. H. Martin, S. Shiraiwa, and G. M. Wallace, *Nucl. Fusion* **60**(3), 036001 (2020).
- A. K. Ram and K. Hizanidis, *Phys. Plasmas* **23**(2), 022504 (2016).
- N. Bertelli, G. Wallace, P. T. Bonoli, R. W. Harvey, A. P. Smirnov, S. G. Baek, R. R. Parker, C. K. Phillips, E. J. Valeo, J. R. Wilson, and J. C. Wright, *Plasma Phys. Controlled Fusion* **55**(7), 074003 (2013).
- Y. Peysson, J. Decker, L. Morini, and S. Coda, *Plasma Phys. Controlled Fusion* **53**(12), 124028 (2011).
- V. P. Ridolfini, M. L. Apicella, G. Calabro, C. Cianfarani, E. Giovannozzi, and L. Panaccione, *Nucl. Fusion* **51**(11), 113023 (2011).
- S. G. Baek, B. Biswas, P. T. Bonoli, D. Brunner, I. C. Faust, A. E. Hubbard, J. W. Hughes, B. LaBombard, R. T. Mumgaard, M. Porkolab, S. Shiraiwa, G. M. Wallace, and S. J. Wukitch, *AIP Conf. Proc.* **2260**, 030006 (2020).
- B. Biswas, S. Gyou Baek, P. Bonoli, S. I. Shiraiwa, G. Wallace, and A. White, *Plasma Phys. Controlled Fusion* **62**(11), 115006 (2020).
- J. Decker, Y. Peysson, J. F. Artaud, E. Nilsson, A. Ekedahl, M. Goniche, J. Hillairet, and D. Mazon, *Phys. Plasmas* **21**(9), 092504 (2014).
- S. G. Baek, B. Biswas, G. M. Wallace, P. T. Bonoli, B. J. Ding, M. H. Li, Y. C. Li, Y. F. Wang, M. Wang, C. B. Wu, G. H. Yan, J. Chen, X. Zhai, A. M. Garofalo, W. Choi, F. Poli, and S. Shiraiwa, *Nucl. Fusion* **61**(10), 106034 (2021).
- C. B. Wu, B. J. Ding, M. H. Li, S. G. Baek, G. M. Wallace, Y. C. Li, G. H. Yan, and S. C. Liu, *Phys. Plasmas* **28**(8), 082507 (2021).
- S. Weinberg, *Phys. Rev.* **126**(6), 1899–1909 (1962).
- T. H. Stix, *The Theory of Plasma Waves* (McGraw-Hill, 1962).
- A. Cardinali, L. Morini, C. Castaldo, R. Cesario, and F. Zonca, *Phys. Plasmas* **14**(11), 112506 (2007).
- A. Cardinali and F. Santini, *Plasma Phys. Controlled Fusion* **53**(12), 125001 (2011).
- M. Brambilla, *Nucl. Fusion* **19**(10), 1343–1357 (1979).
- Y. Peysson and J. Decker, Technical Report No. EUR-CEA-FC-1739 (2008).
- A. P. Smirnov and R. Harvey, *Bull. Am. Phys. Soc.* **40**, 1837 (1995).
- W. Harvey and M. McCoy, in Proceedings of the IAEA Technical Committee Meeting on Simulation and Modeling of Thermonuclear Plasmas (1992).
- R. Cesario, L. Amicucci, A. Cardinali, C. Castaldo, M. Marinucci, F. Napoli, F. Paoletti, D. De Arcangelis, M. Ferrari, A. Galli, G. Gallo, E. Pullara, G. Schettini, and A. A. Tuccillo, *Nucl. Fusion* **54**(4), 043002 (2014).
- W. Horton, M. Goniche, Y. Peysson, J. Decker, A. Ekedahl, and X. Litaudon, *Phys. Plasmas* **20**(11), 112508 (2013).
- A. Kuley and V. K. Tripathi, *Phys. Plasmas* **16**(3), 032504 (2009).

- ³⁷V. Fuchs, P. T. Bonoli, I. P. Shkarofsky, A. Cote, Y. Demers, and C. Janicki, *Nucl. Fusion* **35**(1), 1–22 (1995).
- ³⁸V. PericoliRidolfini, A. Ekedahl, Y. Baranov, J. A. Dobbing, B. Fischer, C. Gormezano, M. Lennholm, F. Rimini, J. Romero, P. Schild, and F. X. Soldner, *Plasma Phys. Controlled Fusion* **39**(7), 1115–1128 (1997).
- ³⁹B. Biswas, S. I. Shiraiwa, S.-G. Baek, P. Bonoli, A. Ram, and A. E. White, *J. Plasma Phys.* **87**(5), 905870510 (2021).
- ⁴⁰A. Kuley, Z. X. Wang, Z. Lin, and F. Wessel, *Phys. Plasmas* **20**(10), 102515 (2013).
- ⁴¹J. Bao, Z. Lin, A. Kuley, and Z. X. Wang, *Nucl. Fusion* **56**(6), 066007 (2016).
- ⁴²T. G. Jenkins, T. M. Austin, D. N. Smithe, J. Loverich, and A. H. Hakim, *Phys. Plasmas* **20**(1), 012116 (2013).
- ⁴³A. Kuley, Z. Lin, J. Bao, X. S. Wei, Y. Xiao, W. Zhang, G. Y. Sun, and N. J. Fisch, *Phys. Plasmas* **22**(10), 102515 (2015).
- ⁴⁴J. Bao, Z. Lin, A. Kuley, and Z. X. Lu, *Plasma Phys. Controlled Fusion* **56**(9), 095020 (2014).